Understanding the power requirements of autonomous underwater systems, Part I: An analytical model for optimum swimming speeds and cost of transport

A.B. Phillips [a], M. Haroutunian [b,*], A.J. Murphy [b], S.W. Boyd [a], J.I.R. Blake [a], G. Griffiths [c]

[a] University of Southampton, Southampton, SO17 1BJ, UK
[b] Newcastle University, Newcastle, NE1 7RU, UK
[c] National Oceanography Centre, University of Southampton Waterfront Campus, Southampton SO14 3ZH, UK

A R T I C L E   I N F O

A B S T R A C T

Many marine species exhibit capabilities that would be desirable for manmade systems operating in the maritime environment. However, without detracting from the potential, if bioinspiration is to prove beneficial, it is important to have a consistent set of metrics that allow fair comparison, without bias, when comparing the performance of engineered and biological systems. In this study we focus on deriving an unbiased metric of performance applicable to marine animals and engineered subsea vehicles for one of the most fundamental of properties; that of the energy cost of locomotion. We present a rational analytical model of the physics behind the total energy cost of locomotion applicable to both biological and engineered autonomous underwater marine systems. This model proposes the use of an equivalent spheroid efficiency as a fair metric to compare engineered and biological systems. The model is then utilised to identify how changes in mass, speed, spheroid efficiency and hotel load impact the performance of the system.

1. Introduction

Biologically inspired swimmers are flourishing with various prototypes of a new generation of biomimicked vehicles being built. These include the "GhostSwimmer" which is being tested by the US Navy (Telepraph, 2014), the "Mantabot" which mimickes the swimming of a ray (Unmanned, 2012) and the Aqua Jelly (jellyfish) developed by Festo (Festo, 2013). Bioinspiration and biomimetics have great potential to lead to new concepts in the design and implementation of engineered artefacts swimming within the oceans (Bandyopadhyay, 2005). Therefore, it is technically relevant to investigate the possible advantages of the systematic design and build of bioinspired vehicles.

The routine activities or missions of both pelagic marine animals and free swimming autonomous underwater vehicles (AUVs) require these systems to transit between multiple locations. For both biological and engineered systems there is an evolutionary or design driver towards reducing the total energy consumption of the system when completing these journeys.

AUVs are almost invariably deployed with a finite energy store; by reducing the energy cost per unit distance travelled the range of the vehicle may be enhanced (e.g. Furlong et al. (2007) and Phillips et al. (2012)). For pelagic species swimming is the only alternative for most animals to find food, escape predators and reproduce successfully (Videler, 1993). Averaged over a period, the amount of energy acquired by an individual through feeding must exceed the amount of energy expended by daily activities, growth and reproduction. Based on optimal foraging theory, natural selection should operate to maximise the ratio of energy income to energy expenditure (Townsend and Winfield, 1985). Hence, the solutions adopted by marine animals to reduce their energetic requirements may provide inspiration to enhance the design of the next generation of free swimming AUVs.

Without detracting from the potential, if bioinspiration is to prove beneficial, it is important to have a consistent set of metrics that allow fair comparison, without bias, when comparing the performance of engineered and biological systems. However, such an unbiased comparator can be elusive given the disparity in the forms of biological and engineered components, even for those that essentially perform the same functions.

For example propulsive efficiency is often quoted by both engineers and biologists as a measure of the ratio of the effective

---

* Corresponding author. Tel.: +0191 208 6104.
  E-mail address: maryam.haroutunian@ncl.ac.uk (M. Haroutunian).

Nomenclature

$(1+k)$	Form factor (–)
$(1-t)$	Thrust Deduction (–)
a	Mass allometric scaling constant for in-water maintenance power (variable)
A	Wetted surface area (m^2)
A_s	Wetted Surface Area of equivalent ellipsoid (m^2)
b	Mass allometric scaling exponent for in-water maintenance power (–)
C_D	Drag coefficient (–)
C_f	Skin friction coefficient (–)
C_v	Viscous drag coefficient (–)
COT	Cost of transport (J/kg/m)
COT_{net}	Net cost of transport (J/kg/m)
COT_{opt}	Optimum Cost of Transport (J/kg/m)
D	Diameter (m)
D_s	Equivalent spheroid Diameter (m)
E	Gravimetric Specific Energy of Power Source (J/kg)
L	Length (m)
L/D_s	Slenderness ratio (–)
m	Mass (kg)
n	Number of samples (–)
P_H	In Water Maintenance power requirement (W)
P_P	Propulsion power requirement (W)
q	Proportion of system mass devoted to energy storage (–)
R	Range (m)
Re	Reynolds number (–)
R_{max}	Maximum range (m)
t	Thrust deduction (–)
U	Forward speed (m/s)
U_{opt}	Optimum speed (m/s)
α	Re scaling constant for skin friction coefficient (–)
β	Re scaling exponent for skin friction coefficient (–)
ε	Spheroid eccentricity (–)
ϕ	Proportion of the system mass devoted to energy storage (–)
ζ	Equivalent spheroid efficiency (–)
ν	Kinematic viscosity (m^2/s)
ρ	Water density (kg/m^3)
τ	Scale factor (–)
η_a	Actuator efficiency (–)
η_p	Propulsive efficiency (–)

power to the power delivered to the propulsion system

$$\eta_p = \frac{Effective\ Power}{Delivered\ Power}. \tag{1}$$

Numerous authors have quoted high propulsive efficiencies, η_p, for marine animals operating at turbulent Reynolds numbers using carangiform and thunniform type propulsion (high speed long-distance swimmers where virtually all movement is in the caudal fin). For example, the propulsive efficiencies of pseudo killer whales at 0.9 (Fish, 1996), bottlenose dolphins at 0.81 (Fish, 1993) and fin whale at 0.85 (Bose and Lien, 1989) are high compared with those of a typical propeller (Wageningen B5-75) open water efficiency of 0.5 to 0.7 (Carlton, 2007).

However, these results must be treated with caution. The action of any propulsor, be it an oscillating foil, propeller or water jet, will locally modify the flow around the individual. In turn modifying the resistance of a self-propelled individual compared to a towed (or passive) individual. There is inconsistency between the standard methods for accounting for this change in resistance (typically an increase) between biological and engineered systems.

For ships the increase in self-propelled resistance is included as part of the propulsive efficiency rather than as an increment on the drag. Thus the propulsive efficiency of an AUV is:

$$\eta_{p(engineering)} = \frac{Towed\ Resistance \times Velocity}{Propulsive\ Power\ to\ Shaft}. \tag{2}$$

While not universally accepted, in biology the influence of the propulsor on the 'drag' is often considered as an added resistance factor, λ, which is the ratio of the swimming thrust to passive drag:

$$\lambda = \frac{Swimming\ Thrust}{Passive\ Drag}. \tag{3}$$

The added resistance factor is highly dependent on propulsive mode and accounts for drag increases due to large-amplitude lateral body movements that modify the water flow in the boundary layer and around the body, resulting in increased frictional and form drag (Webb, 1975). Experimental data collected by Webb (1975) shows that the drag coefficient for fish swimming at high Reynolds numbers can be up to four times that of a rigidly gliding fish. Importantly this added resistance is typically not included in the propulsive efficiency. Hence the propulsive

efficiency of a marine animal is often taken to be:

$$\eta_{p(biology)} = \frac{Swimming\ Thrust \times Velocity}{Power\ in\ wake}. \tag{4}$$

There are sound reasons for the differing approaches due to the measurement techniques available for engineered and biological systems (Webb, 1975). However, the consequence is that direct comparison of quoted propulsive efficiencies between engineered and biological systems is biased towards biological systems since biological values do not incorporate the added resistance due to the movement of the body. To enable a fair comparison:

$$\eta_{p(engineering)} = \frac{\eta_{p(biology)}}{\lambda}. \tag{5}$$

In this work a combination of reduced-complexity analytical formulations and dimensional analysis is used to generate a comprehensive idealised analytical model of the cost of transport and optimum swimming speed of an individual, be it a biological or engineered system based on system metrics including equivalent spheroid efficiency. The analytical model provides enhanced understanding of the implications of propulsion and non-propulsion power requirements on the energetic performance of individuals. In Part II of this paper this understanding is used to explain trends in collated published swimming performance data, where a number of recent biological studies on individual species (Behrens et al., 2006; Clark and Seymour, 2006; Fitzgibbon et al., 2007; Korsmeyer et al., 2002; Ohlberger et al., 2006; Otani et al., 2001; Palstra et al., 2008; Rosen and Trites, 2002; Steinhausen et al., 2005; Tanaka et al., 2001; Tudorache et al., 2011; Williams and Noren, 2009) have allowed the creation of a significantly larger data sets than considered by previous comparative studies, e.g. Videler (1993) and Videler and Nolet (1990).

2. Analytical model

Due to the limited availability of energetic data for marine animals, empirical models have been previously proposed to supplement and enhance our understanding. Previous studies have developed equations for the optimum cost of transport and/or optimum swimming speed of marine animals using regression

analysis (Videler, 1993; Videler and Nolet, 1990; Williams, 1999) or else using combinations of dimensional analysis and other modelling techniques (Bejan and Marden, 2006; Hedenström, 2003; Watanabe et al., 2010; Weihs, 1973). While Williams (2010) developed a mission-specific model for the energy expenditure and range of AUVs, none of the existing approaches are suitable for comparing biological and engineered systems. The model presented here is a significant extension and generalisation of the models of Watanabe et al. (2010) and Weihs (1973) to make it applicable for laminar and turbulent flow and biological and engineered systems.

The approach is not intended to account for all forms of biological or engineering variation; rather it is intended to provide a framework for understanding general tendencies and relationships, and to provide a means to explore potentially interesting areas, the incorporation of an equivalent spheroid efficiency is proposed to allow fair comparison between both engineered and biological systems. For both biological and engineered systems typically only limited data is available, consequently this is reflected in the set of key parameters.

2.1. Equivalent spheroid

Reduced complexity models are used in many areas of science to gain insight into what is important and what is not, before moving to more representative modelling. We reduce complexity in our model by assuming that the form of the biological or engineered system corresponds to that of an equivalent spheroid, defined as a neutrally buoyant prolate spheroid with the same length and mass as the individual, the equivalent diameter can be determined from,

$$D_S = \sqrt{\frac{6m}{\rho\pi L}} \tag{6}$$

while the surface area is determined from,

$$A_s = 2\pi \frac{D_S^2}{4}\left(1 + \frac{L}{D_S \varepsilon}\sin^{-1}\varepsilon\right), \tag{7}$$

where

$$\varepsilon = \sqrt{1 - \frac{D_S^2}{L^2}} \tag{8}$$

Such an assumption allows estimates to be made of key parameters including diameter or wetted surface area, which, for animals and engineered systems, are often not reported. Fig. 1 illustrates the differences between the actual and the modelled parameters when displacement and length are constrained to be equal.

The assumption that the individual may be represented as a prolate spheroid allows predictions to be made regarding the energetic costs of an individual. To make the analytical model generic each equivalent spheroid will be defined by its mass and its slenderness ratio, $\frac{L}{D_s}$. Thus the length is given by,

$$L = cm^{1/3}, \tag{9}$$

where,

$$c = \left(\frac{6\left(\frac{L}{D_s}\right)^2}{\rho\pi}\right)^{1/3}. \tag{10}$$

Note c is a constant for geometrically similar spheroids operating in the same fluid. The wetted surface area can be approximated by,

$$A_s \approx dm^{\frac{2}{3}}, \tag{11}$$

where,

$$d = \left(\frac{1}{\rho}\right)^{2/3}\left(-0.0122\left(\frac{L}{D_S}\right)^2 + 0.5196\frac{L}{D_S} + 4.2732\right). \tag{12}$$

Again d is a constant for geometrically similar spheroids operating in the same fluid. For $1.1 > L/D_S < 15$ this approximation gives an error of less than 1% of the exact wetted surface area derived from Eq. (7), this range of L/D_S encompasses the majority of pelagic marine animals and survey style AUVs (Murphy and Haroutunian, 2011).

2.2. In-water maintenance power

The total powering requirements of the idealised system can be derived be modelling the in-water maintenance costs and the propulsion power requirements. The in water-maintenance cost will be represented by a power function,

$$P_H = am^b, \tag{13}$$

where a is a constant of proportionality, m is the system mass and b is the allometric scaling exponent. Such a relationship is commonly used to represent the relationship between body mass and energy metabolism in animals (Heusner, 1985). It will be shown in Section 4.1 that such an assumption is also reasonable for engineered systems.

2.3. Propulsion power

Dimensional analysis and common engineering practice state that the total propulsion power (i.e the power drawn by the entire propulsion system including actuators) of a deeply submerged

Delphin2
Length, L=1.96m
Displacement, m=72 kg
Max Diameter, D=0.254m
Wetted Surface Area, A=1.42m^2
Slenderness Ratio, L/D=7.7

Equivalent Spheroid
Length, L=1.96m
Displacement, m=72 kg
Diameter, Ds=0.262 m
Wetted Surface Area, As=1.3m^2
Slenderness Ratio, L/Ds=7.5

Dolphin (Hui, 1987)
Length, L=1.73m
Displacement, m=59.2kg
Max Diameter, D=0.31 m
Wetted Surface Area, A=1.04m^2
Slenderness Ratio, L/D=5.6

Equivalent Spheroid
Length, L=1.73m
Displacement, m=59.2 kg
Diameter, Ds=0.25 m
Wetted Surface Area, As=1.06m^2
Slenderness Ratio, L/Ds=6.92

Fig. 1. Equivalent spheroid examples for an underwater vehicle (Delphin2 Phillips et al. (2013) and Steenson et al. (2014)) and a marine mammal (picture by NOAA) illustrating the differences between the actual and the modelled parameters when displacement and length are constrained to be equal (Dolphin, Hui, 1987).

individual can be determined from:

$$P_P = \frac{\rho}{2\eta_a\eta_p}C_DAU^3 \qquad (14)$$

where, ρ is the fluid density, C_D is the drag coefficient of a towed (or passive) system, A is the wetted surface area of the system, η_a is the actuator efficiency and η_p is the propulsive efficiency. Using a similar argument the power requirement of a 100% efficient equivalent spheroid, P_{P_S}, may be calculated from

$$P_{P_S} = \frac{\rho}{2}C_{D_S}A_sU^3, \qquad (15)$$

where C_{D_S} is the drag coefficient, and A_s the wetted surface area of the equivalent spheroid.

2.4. Equivalent spheroid efficiency

Defining the equivalent spheroid efficiency, ζ, as the ratio of the power required to propel a 100% efficient equivalent spheroid to the power required by a real individual at the same speed,

$$\zeta = \frac{P_{P_S}}{P_P} = \eta_a\eta_p\frac{C_{D_S}A_s}{C_DA} \qquad (16)$$

ζ includes both hydrodynamic and actuator efficiency, it also makes allowance for the difference in drag coefficient and wetted surface area between the real system and an equivalent spheroid. Thus the propulsion power can be represented by,

$$P_P = \frac{\rho}{2\zeta}C_{D_S}A_sU^3. \qquad (17)$$

For this study we will assume that the equivalent spheroid efficiency is invariant to forward speed. We will also assume that neither ρ or A_s have any dependency on the other variables considered in this study. The use of equivalent spheroid efficiency allows fair comparison between engineered and biological systems, where only limited data is available. To calculate the only system specific information required are length, mass and propulsion power at a set speed.

2.5. Drag coefficient prediction

Based on the methodologies of Hughes developed for scaling of drag components of ships, the drag of a deeply submerged spheroid experiencing only viscous drag, C_v, may be represented by,

$$C_{D_S} = C_v = C_f(1+k) \qquad (18)$$

where C_f is the skin friction coefficient based on flat plate results, while the $(1+k)$ is a form factor dependent on hull form to account for the viscous pressure resistance (Molland et al., 2011). The standard skin friction lines for laminar flow (Blasius line) and turbulent flow (von Karman line) past a flat plate are of the form,

$$C_f = \alpha Re^\beta, \qquad (19)$$

where the constant, α, and the exponent, β, are flow regime dependent and, Re, is the length based Reynolds number. The form factor $(1+k)$ of an spheroid can be predicted empirically from Hoerner (1965),

$$(1+k) = 1 + 1.5\left(\frac{L}{D_S}\right)^{-3/2} + 7\left(\frac{L}{D_S}\right)^{-3}. \qquad (20)$$

Substituting Eqs. (19)–(21) into (18) the propulsion power requirement is given by

$$P_P = \frac{e}{\zeta}\alpha m^{\frac{\beta+2}{3}}U^{(3+\beta)}, \qquad (21)$$

where

$$e = \frac{\rho}{2}(1+k)\frac{c^\beta}{\nu^\beta}d. \qquad (22)$$

e is constant for geometrically similar individuals operating in the same fluid.

2.6. Optimum cost of transport

One widely accepted metric used to compare the energetic performance of different animals is cost of transport, COT (Schmidt-Nielsen, 1972; Tucker, 1970; Videler, 1993). COT is a normalised measure of the energy required to transport the mass m of an individual, over a unit distance at a speed U. The general formulation of cost of transport for an individual is given by:

$$COT = \frac{P_H + P_P}{mU}. \qquad (23)$$

Where P_H, is the power expended to operate or sustain the animal's non-propulsion systems, and P_P is the power associated with propulsion. At this level of abstraction there is almost a one-to-one correspondence with engineered systems. For engineered systems the power expended on non-propulsion systems is often referred to as the hotel load and is associated with powering computers, hard drives and all the sensors required to provide functions equivalent to those of an animal, such as knowing orientation and position, and condition monitoring. This is equivalent to the in-water maintenance cost of a marine animal while at rest associated with blood flow, respiration etc. However, the hotel load in an underwater vehicle can be defined to include the power consumed by the instruments carried as payload, such as those to make measurements of the environment. Payload power consumption can be similar to, or can exceed, the power required for maintaining the vehicle's core systems. Consequently, in this study, because there is no animal equivalent, payload power consumption is excluded.

The energetic costs of propulsion, P_P, of an individual, animal or underwater vehicle, is as a direct result of generating thrust to overcome fluid dynamic drag. The energy required is influenced by a variety of environmental factors, such as water temperature and salinity, propulsion methods and associated efficiency as well as physiological and morphological characteristics of the system (Allen et al., 2000; Hammer, 1995; Lighthill, 1969).

Substituting Eqs. (13) and (21) into Eq. (23) the cost of transport for an equivalent spheroid is:

$$COT = \frac{P_H + P_P}{mU} = \frac{am^b + \frac{e}{\zeta}\alpha m^{\frac{\beta+2}{3}}U^{(3+\beta)}}{mU} \qquad (24)$$

COT versus swimming speed results in a 'U' shaped function, see Fig. 2, the optimum swimming speed, U_{opt} associated with the minimum cost of transport COT_{opt} may be established by differentiating Eq. (24) with respect to U, then setting the result equal to zero to find the global minimum and then rearranging for U_{opt},

$$U_{opt} = \left(\frac{a\zeta}{(2+\beta)e\alpha}\right)^{\frac{1}{3+\beta}} m^{\frac{3b-\beta-2}{9+3\beta}} \qquad (25)$$

Multiplying out the brackets and gathering like terms,

$$U_{opt} = \underbrace{a^{\frac{1}{3+\beta}}}_{I} \times \underbrace{\zeta^{\frac{1}{3+\beta}}}_{II} \times \underbrace{e^{-\frac{1}{3+\beta}}}_{III} \times \underbrace{\alpha^{-\frac{1}{3+\beta}} \times (2+\beta)^{-\frac{1}{3+\beta}}}_{IV} \times \underbrace{m^{\frac{3b-\beta-2}{9+3\beta}}}_{V} \qquad (26)$$

With the equation in this form it is possible to identify how the key model parameters influence the optimum swimming speed. In the preceding equation, term I shows that U_{opt} varies with a (the mass coefficient used in determining the in-water maintenance cost) raised to the power $\frac{1}{3+\beta}$. This exponent will thus vary

depending on the flow regime. For laminar flow $\beta = -0.5$, while for turbulent flow $\beta = -0.2$, thus U_{opt} will be more slightly more sensitive to variations in a and thus in-water propulsion requirements when operating in a turbulent flow regime than in a laminar one. Similar arguments can be made for terms II and III. Term IV is only dependent on flow regime. Term V demonstrates how the scaling exponent on m is dependent on the allometric mass scaling exponent b as well as the flow regime.

Note that by differentiating Eq. (24) with respect to speed it can be shown that the propulsion power at the optimum swimming speed can be related to the non-propulsion power requirement by,

$$P_H = am^b = (2+\beta)\frac{e}{\zeta}\alpha m^{\frac{\beta+2}{3}} U_{opt}^{(3+\beta)} = (2+\beta)P_{PU=U_{opt}} \tag{27}$$

This ratio is independent of all other parameters, thus the power consumption at the optimum speed is a function of in-water maintenance power requirements, P_H, and the exponent on Reynolds number for the skin friction calculation, β. For vehicles operating in the same flow regime (laminar or turbulent) the propulsion power, P_P, at U_{opt} is only a function of the in-water

propulsion power requirement. Thus the optimum cost of transport becomes,

$$COT_{opt} = \frac{P_H + P_{PU=U_{opt}}}{mU_{opt}} = \frac{\left(1+\frac{1}{2+\beta}\right)P_H}{mU_{opt}}. \tag{28}$$

Substituting the result for U_{opt} Eq. (25) into Eq. (28), the optimum cost of transport is given by:

$$COT_{opt} = a\left(1+\frac{1}{2+\beta}\right)\left(\frac{(2+\beta)e\alpha}{a\zeta}\right)^{\frac{1}{3+\beta}} m^{\frac{6b+3b\beta-2\beta-7}{9+3\beta}}. \tag{29}$$

2.7. Maximum range

For AUVs with a finite energy store or marine animals which migrate without feeding, the maximum range, R_{max}, can be determined as,

$$R_{max} = \frac{E\phi m}{mCOT_{opt}}, \tag{30}$$

where E is the specific energy of the power source in (J/kg) and ϕ is the proportion of the system mass devoted to energy storage (0 corresponds to 0% of the mass while 1 corresponds to 100%).

2.8. Operation at non-optimum speeds

While the optimum swimming speed is energetically optimum, other mission constraints may lead the individual to operate at speeds above or below the optimum i.e. sprinting to overcoming currents or to capture prey, or slowing to a stop to interact with the environment. The impact of operating at speeds other than U_{opt} can be derived relative to the optimum values, let $\tau = U/U_{opt}$,

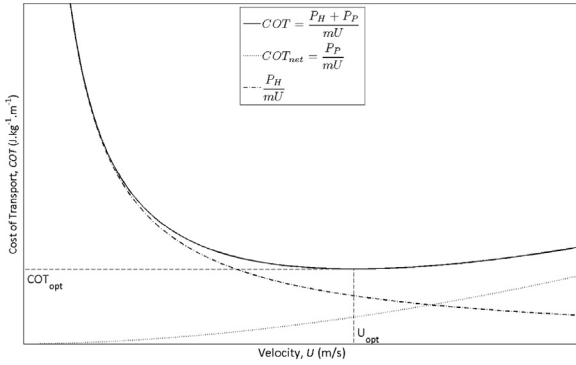$$COT = COT_{opt}\frac{2+\beta+\tau^{(3+\beta)}}{(3+\beta)\tau}, \tag{31}$$

Fig. 2. Idealised cost of transport curve. The net cost of transport, COT_{net}, is often defined as the component of the cost of transport associated with propulsion.

Table 1
Key results from analytical model.

	Laminar flow model (Blasius skin friction line)		Turbulent flow model (Prandtl–Von Kármán skin friction line)	
In water maintenance power, P_H	am^b			(13)
Skin friction coefficient, C_f	$1.327Re^{-1/2}$	(34)	$0.072Re^{-1/5}$	(35)
Propulsion power, P_P	$1.327\frac{e}{\zeta}m^{1/2}U^{5/2}$	(36)	$0.072\frac{e}{\zeta}m^{3/5}U^{2.8}$	(37)
Geometric and fluid constants	$e = \frac{\rho}{2}(1+k)\frac{c^{-1/2}}{\nu^{-1/2}}d$	(38)	$e = \frac{\rho}{2}(1+k)\frac{c^{-1/5}}{\nu^{-1/5}}d$	(39)
	$c = \left(\frac{6(\frac{L}{D})^2}{\rho\pi}\right)^{1/3}$			(10)
	$d = \left(\frac{1}{\rho}\right)^{\frac{2}{3}}\left(-0.0122\left(\frac{L}{D_S}\right)^2 + 0.5196\frac{L}{D_S} + 4.2732\right)$			(12)
	$(1+k) = 1 + 1.5\left(\frac{L}{D_S}\right)^{-3/2} + 7\left(\frac{L}{D_S}\right)^{-3}$			(20)
Cost of transport, COT	$\frac{am^b + 1.327\frac{e}{\zeta}m^{1/2}U^{5/2}}{mU}$	(40)	$\frac{am^b + 0.072\frac{e}{\zeta}m^{3/5}U^{2.8}}{mU}$	(41)
Optimum speed, U_{opt}	$\left(\frac{a\zeta}{1.9905e}\right)^{2/5}m^{\frac{2b-1}{5}}$	(42)	$\left(\frac{a\zeta}{0.1296e}\right)^{1/2.8}m^{\frac{b-3/5}{2.8}}$	(43)
Optimum cost of transport, COT_{opt}	$2.195a^{\frac{3}{5}}\left(\frac{e}{\zeta}\right)^{\frac{2}{5}}m^{\frac{3b-4}{5}}$	(44)	$0.750a^{\frac{9}{14}}\left(\frac{e}{\zeta}\right)^{\frac{5}{14}}m^{\frac{9b-11}{14}}$	(45)
Propulsion power at optimum speed, $P_{P_{u=u_{opt}}}$	$\frac{P_H}{1.5}$	(46)	$\frac{P_H}{1.8}$	(47)
Maximum range, R_{max}	$0.455E\phi a^{-\frac{3}{5}}\left(\frac{\zeta}{e}\right)^{\frac{2}{5}}m^{\frac{4-3b}{5}}$	(48)	$1.334E\phi a^{-\frac{9}{14}}\left(\frac{\zeta}{e}\right)^{\frac{5}{14}}m^{\frac{11-9b}{14}}$	(49)

Table 2
Proportionality relationships between key model parameters and COT_{opt}, R_{max} and U_{opt}, values in brackets are for laminar flow.

Parameter	In-water maintenance power, P_H	Equivalent spheroid efficiency, ζ	Mass and allometric scaling exponent, m and b	Total stored energy, $E\phi$
Optimum cost of transport, COT_{opt}	$P_H^{9/14}$	$\zeta^{5/14}$	$m^{\frac{9b-11}{14}}$	$\sim$
	$\left(P_H^{3/5}\right)$	$\left(\zeta^{2/5}\right)$	$\left(m^{\frac{3b-4}{5}}\right)$	$\sim$
Maximum range R_{max}	$P_H^{-9/14}$	$\zeta^{-5/14}$	$m^{\frac{11-9b}{14}}$	$E\phi$
	$\left(P_H^{-3/5}\right)$	$\left(\zeta^{-2/5}\right)$	$\left(m^{\frac{4-3b}{5}}\right)$	$(E\phi)$
Optimum speed U_{opt}	$P_H^{5/14}$	$\zeta^{-5/14}$	$m^{\frac{b-0.6}{2.8}}$	$\sim$
	$\left(P_H^{2/5}\right)$	$\left(\zeta^{-2/5}\right)$	$\left(m^{\frac{b-0.5}{2.5}}\right)$	$\sim$

$$R = R_{max}\frac{(3+\beta)\tau}{2+\beta+\tau^{(3+\beta)}}, \qquad (32)$$

$$P_P = \frac{P_H\tau^{(3+\beta)}}{2+\beta}. \qquad (33)$$

2.9. Transition from laminar to turbulent flow

For this study we will consider two skin friction lines: the Blasius skin friction line for laminar flow and the Prandtl–Von Kármán skin friction line for turbulent flows (Comstock, 1977), the key results using these relationships are tabulated in Table 1.

The transition from laminar flow to turbulent flow is a complex phenomenon which will not be discussed in detail here. For the purposes of this study we have assumed that laminar flow is prevalent up to Reynolds numbers of 500,000 and that fully turbulent flow is developed after Reynolds numbers of 1,000,000. For
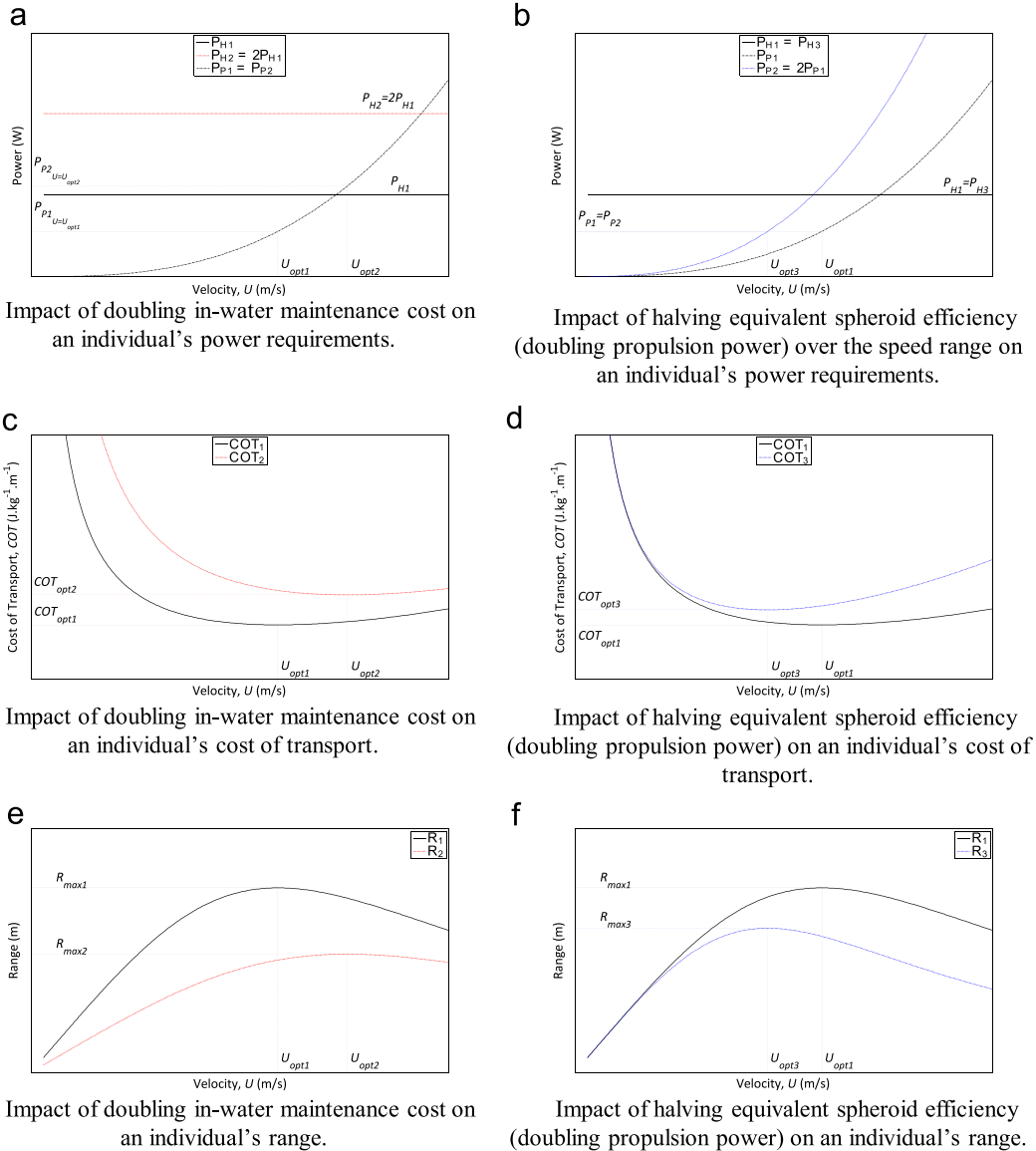
a

Impact of doubling in-water maintenance cost on an individual's power requirements.

b

Impact of halving equivalent spheroid efficiency (doubling propulsion power) over the speed range on an individual's power requirements.

c

Impact of doubling in-water maintenance cost on an individual's cost of transport.

d

Impact of halving equivalent spheroid efficiency (doubling propulsion power) on an individual's cost of transport.

e

Impact of doubling in-water maintenance cost on an individual's range.

f

Impact of halving equivalent spheroid efficiency (doubling propulsion power) on an individual's range.

Fig. 3. Impact of variations in in-water maintenance cost or propulsion power requirement on optimum cost of transport optimum speed and maximum range. Figures are to scale for the turbulent flow case. (a) Impact of doubling in-water maintenance cost on an individual's power requirements, (b) impact of halving equivalent spheroid efficiency (doubling propulsion power) over the speed range on an individual's power requirements, (c) impact of doubling in-water maintenance cost on an individual's cost of transport, (d) impact of halving equivalent spheroid efficiency (doubling propulsion power) on an individual's cost of transport, (e) impact of doubling in-water maintenance cost on an individual's range, (f) impact of halving equivalent spheroid efficiency (doubling propulsion power) on an individual's range.

$500,000 < Re < 1,000,000$ we have used a linear function to smooth between the results for the laminar and turbulent models.

3. Analytical model findings

The analytical model allows the relative importance of each parameter on the energy expenditure of an autonomous underwater system. By definition a is proportional to in-water maintenance cost and ζ is a measure of the hydrodynamic and propulsion efficiency of the individual, the impact of changes in these variables on COT_{opt}, R_{max} and U_{opt} may be explored. Table 2 highlights the key results of this analysis for laminar and turbulent flow, showing the relative importance of the key parameters and their influence on the measures of COT_{opt}, R_{max} and U_{opt}.

The impact of doubling the systems in-water maintenance cost or the equivalent spheroid efficiency over the speed range are considered in Fig. 3.

For turbulent flow, doubling the in-water maintenance costs results in the cost of transport rising by a factor of $2^{9/14}$ (56%), while the maximum range is reduced by $2^{-9/14}$ (36%). The optimum swimming speed rises by a factor of $2^{5/14}$ (28%). At the optimum swimming speed the ratio of the in water maintenance load and propulsion load is constant (Eq. (27)), therefore as the in water maintenance load doubles so does the propulsion power at the optimum swimming speed.

Doubling the propulsion power requirements over the speed range results in the optimum swimming speed reducing by a factor of $2^{-5/14}$ (22%), the reduction in optimum speed is such that the propulsion power at the optimum speed is constant for both cases. While the power consumption is constant, the reduction in the optimum swimming speed increases the optimum cost of transport, rising by a factor of $2^{5/14}$ (28%), while the maximum range is reduced by $2^{-5/14}$ (22%).

3.1. Influence of system mass on optimum cost of transport

It is convention to present optimum cost of transport and optimum swimming speed versus mass when comparing different individuals. To examine how optimum swimming speed varies with respect to mass, partially differentiate Eq. (25) with respect to mass,

$$\frac{\partial U_{opt}}{\partial m} = \left(\frac{3b-\beta-2}{9+3\beta}\right)\left(\frac{a\zeta}{(2+\beta)e\alpha}\right)^{\frac{1}{3+\beta}} \times m^{\frac{3b-\beta-3}{9+3\beta}}. \tag{50}$$

For geometrically similar systems with the same equivalent spheroid efficiency this may be approximated by an equation of the form $\frac{\partial U_{opt}}{\partial m} = fm^g$ where f is a positive constant. Consequently, the sign of the gradient of the U_{opt} versus mass line is governed by the value of scaling exponent in Eq. (50) which is dependent on the maintenance power allometric scaling exponent, b and scaling exponent on Reynolds number to determine the skin friction coefficient β. For laminar flow $\beta = -0.5$:

$$\frac{\partial U_{opt}}{\partial m} = \begin{cases} > 0 & for \quad b > 1/2 \\ 0 & for \quad b = 1/2 \\ < 0 & for \quad b < 1/2 \end{cases}. \tag{51}$$

While for turbulent flow $\beta = -0.2$ giving the result is

$$\frac{\partial U_{opt}}{\partial m} = \begin{cases} > 0 & for \quad b > 3/5 \\ 0 & for \quad b = 3/5 \\ < 0 & for \quad b < 3/5 \end{cases}. \tag{52}$$

Similarly the impact of b on the gradient of the optimum cost of transport versus mass curve is also highly informative, by
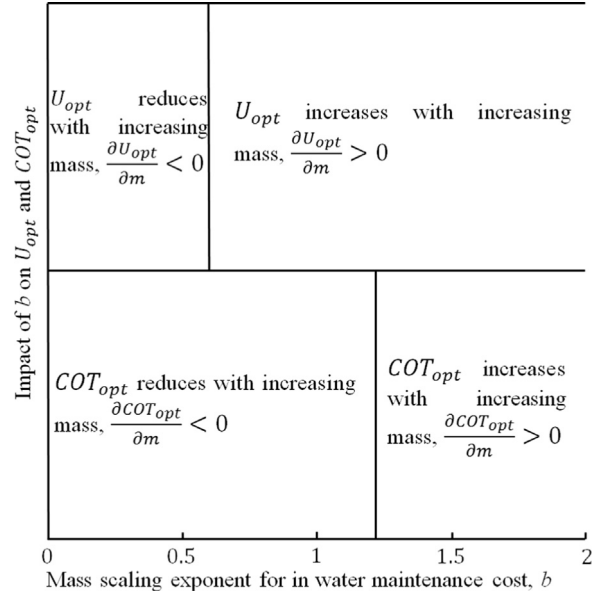

Fig. 4. Impact of mass scaling exponent for the in water maintenance power requirements (for turbulent flow).

differentiating Eq. (29) with respect to mass for laminar flow

$$\frac{\partial COT_{opt}}{\partial m} = \begin{cases} > 0 & for \quad b > 12/9 \\ 0 & for \quad b = 12/9 \\ < 0 & for \quad b < 12/9 \end{cases}. \tag{53}$$

While for turbulent flow the result is

$$\frac{\partial COT_{opt}}{\partial m} = \begin{cases} > 0 & for \quad b > 11/9 \\ 0 & for \quad b = 11/9 \\ < 0 & for \quad b < 11/9 \end{cases}. \tag{54}$$

The above results are illustrated in Fig. 4, for turbulent flow. Dependent on the value of b, three cases can be identified assuming that the system transits at its optimum speed:

- Case 1: $b < 3/5$ for turbulent flow and $b < 1/2$ for laminar flow – Optimum swimming speed reduces with increasing mass while optimum cost of transport reduces with increasing mass. More massive systems will swim slower but have lower energetic costs per unit mass.
- Case 2: $3/5 < b < \frac{11}{9}$ for turbulent flow and $0.5 < b < 12/9$ for laminar flow – Optimum swimming speed increases with increasing mass while optimum cost of transport reduces with increasing mass. More massive individuals will swim faster but have lower energetic costs per unit mass.
- Case 3: $b > 11/9$ for turbulent flow and $b > 12/9$ for laminar flow – Optimum swimming speed reduces with increasing mass while optimum cost of transport reduces with increasing mass. More massive systems will swim faster and have higher energetic costs per unit mass.

While it has been argued that an allometric scaling exponent b, of 3/4 is valid for all animals (Smil, 2000), other authors argue for a value of 2/3 (White and Seymore, 2003). Agutter and Wheatley (2004) review the proposed justifications for the different values. The limitations of the universal scaling law are discussed in detail in Glazier (2005). For pelagic marine species Glazier (2006) argues that the interspecific and intraspecific scaling exponent is variable lying in the range $(1/2 < b < 11/10)$.

For marine animals one might hypothesis that Case 2 provides an evolutionary driver for marine animals to grow more massive,

since they may achieve higher optimum swimming velocities for a lower energetic cost per unit mass. Most of the values for *b* proposed in the studies and reviews fall into this case.

Case 3 would restrict the evolutionary advantage of increasing mass, since the energetic cost per unit mass would increase for an animal swimming at its optimum speed. None of the animal studies suggest *b* values sufficiently high to fall into this case. Case 1 provides an energetic advantage, yet assuming pelagic animals choose to swim at their optimum speed, more massive animals would swim more slowly eventually reaching planktonic speeds (unable to overcome natural currents). The range of *b* values proposed by Glazier (2006) suggest that *b* can be low enough to fall into this case.

4. Conclusion

For pelagic marine animals and underwater vehicles, minimising their cost of transport by swimming at their optimum speed allows them to maximise their range given a finite store of energy. Marine animals with low cost of transport have developed a combined morphology and kinematics of swimming that may lead to the design of bioinspired long range underwater vehicles with enhanced performance. However, given that there are inherent difficulties when seeking to compare engineered and biological systems, there must be a rational basis for selecting which characteristics and which animals to use as the basis for inspiration. In this paper we present a well rationalised analytical model of the physics behind the total energetic cost of locomotion applicable to both biological and engineered autonomous underwater marine systems. The model incorporates the use of an equivalent spheroid efficiency as a fair metric to compare engineered and biological systems. This can be readily calculated from typically available data. To calculate equivalent spheroid efficiency the only system specific information required are length, mass and propulsion power at a set speed. Results from the model are used to provide useful insights into the scaling of common performance metrics with respect to system mass, such as cost of transport and maximum range. The analysis in this work are based upon swimming speeds and energy consumption. Therefore, the scaling considers a combination of drag, thrust and "hull" efficiency as a complete system. As a result it would be possible to make a judgement on the performance of a swimming system. In addition, the analytical model provides a physics-based selection tool to help with selecting candidate marine animal species for bioinspiration, and biologists can use this approach to help understand the observed performance of marine animals.

In Part II we demonstrate how engineers can use the model to facilitate an understanding of biological systems to improve engineered vehicles by comparing the in-service implications of design choices for vehicles.

Acknowledgements

References

Agutter, P.S., Wheatley, D.N., 2004. Metabolic scaling: consensus or controversy? Theor. Biol. Med. Model. 1, 1–13.

Allen, B., Vorus, W.S., Prestero, T., 2000. Propulsion system performance enhancements on REMUS AUVs, OCEANS 2000 MTS/IEEE Conference and Exhibition Providence. RI, USA.

Bandyopadhyay, P.R., 2005. Trends in biorobotic autonomous undersea vehicles. Ocean. Eng. 30 (1), 109–139.

Behrens, J.W., Præbel, K., Steffensen, J.F., 2006. Swimming energetics of the Barents Sea capelin (Mallotus villosus) during the spawning migration period. J. Exp. Mar. Biol. Ecol. 331, 208–216.

Bejan, A., Marden, J.H., 2006. Unifying constructal theory for scale effects in running, swimming and flying. J. Exp. Biol. 209, 238–248.

Bose, N., Lien, J., 1989. Propulsion of a fin whale (Balaenoptera physalus): why the fin whale is a fast swimmer. Proc. R. Soc. Lond. Ser. B, Biol. Sci. 237 (1287), 175–200.

Carlton, J., 2007. Marine Propellers and Propulsion. Butterworth-Heinemann, Oxford.

Clark, T.D., Seymour, R.S., 2006. Cardiorespiratory physiology and swimming energetics of a high-energy-demand teleost, the yellowtail kingfish (Seriola lalandi). J. Exp. Biol. 209, 3940–3951.

Comstock, J.P., 1977. Principles of Naval Architecture, 4th Edition ed. SNAME, New York.

Festo, 2013. AquaJellies 2.0 – Autonomous behaviour in a collective.

Fish, F.E., 1993. Power output and propulsive efficiency of swimming bottlenose dolphins (Tursiops truncatus). J. Exp. Biol. 185, 179–193.

Fish, F.E., 1996. Transitions from drag-based to lift-based propulsion in mammalian swimming. Am. Zool. 36, 628–641.

Fitzgibbon, Q.P., Strawbridge, A., Seymour, R.S., 2007. Metabolic scope, swimming performance and the effects of hypoxia in the mulloway, Argyrosomus japonicus (Pisces: Sciaenidae). Aquaculture 270, 358–368.

Furlong, M.E., McPhail, S.D., Stevenson, P., 2007. A concept sesign for an ultra-long-range survey class AUV, Oceans 07, Aberdeen.

Glazier, D.S., 2005. Beyond the '3/4-power law': variation in the intra- and inter-specific scaling of metabolic rate in animals. Biol. Rev. 80 (1), 611–662.

Glazier, D.S., 2006. The 3/4-power law is not universal: evolution of isometric, ontogenetic metabolic scaling in pelagic animals. BioScience 56 (4), 325–332.

Hammer, C., 1995. Fatigue and exercise tests with fish. Comp. Biochem. Physiol. Part A: Physiol. 112 (1), 1–20.

Hedenström, A., 2003. Scaling migration speed in animals that run, swim and fly. J. Zool., Lond. 259, 155–160.

Heusner, A.A., 1985. Body size and energy metabolism. Annu. Rev. Nutr. 5, 267–293.

Hoerner, S.F., 1965. Fluid-Dynamic Drag, 2nd Edition ed Published by the Author.

Hui, C.A., 1987. Power and Speed of swimming dolphins. J. Mammal. 68 (1), 126–132.

Korsmeyer, K.E., Steffensen, J.F., Herskin, J., 2002. Energetics of median and paired fin swimming, body and caudal fin swimming, and gait transition in parrotfish (Scarus schlegeli) and triggerfish (Rhinecanthus aculeatus). J. Exp. Biol. 205, 1253–1263.

Lighthill, M.J., 1969. Hydromechanics of aquatic animal propulsion. Annu. Rev. Fluid Mech. 1, 413–446.

Molland, A.F., Turnock, S.R., Hudson, D.H., 2011. Ship Resistance and Propulsion. Cambridge University Press, Cambridge.

Murphy, A.J., Haroutunian, M., 2011. Using bio-inspiration to improve the capabilities of underwater vehicles. In: Proceeding of the 17th International Symposium on Unmanned Untethered Submersible Technology (UUST). Portsmouth, Massachusetts, USA.

Ohlberger, J., Staaks, G., Hölker, F., 2006. Swimming efficiency and the influence of morphology on swimming costs in fishes. J. Comp. Physiol. B: Biochem. Syst., Environ. Physiol. 176 (1), 17–25.

Otani, S., Naito, Y., Kato, A., Kawamura, A., 2001. Oxygen consumption and swim speed of the harbor porpoise Phocoena phocoena. Fish. Sci. 67, 894–898.

Palstra, A., van Ginneken, V., van den Thillart, G., 2008. Cost of transport and optimal swimming speed in farmed and wild European silver eels (Anguilla anguilla). Comp. Biochem. Physiol. Part A: Mol. Integr. Physiol. 151 (1), 37–44.

Phillips, A.B., Haroutunian, M., Man, S.K., Murphy, A.J., Boyd, S.W., Blake, J.I.R., Griffiths, G., 2012. Nature in engineering for monitoring the oceans: comparison of the energetic costs of marine animals and AUVs. In: Roberts, G.N., Sutton, R. (Eds.), Further Advances in Unmanned Marine Vehicles. IET, pp. 373–405.

Phillips, AB., Steenson, LV., Rogers, E., Turnock, SR., Harris, CA., Furlong, M.E., 2013. Delphin2: an over actuated autonomous underwater vehicle for manoeuvring research. Int. J. Marit. Eng. 155, 171–180.

Rosen, D.S., Trites, A., 2002. Cost of transport in steller sea lions, Eumetopias jubatus. Mar. Mammal. Sci. 18 (2), 513–524.

Schmidt-Nielsen, K., 1972. Locomotion: energy cost of swimming, flying, and running. Science 177 (4045), 222–228.

Smil, V., 2000. Laying down the law Every living thing obeys the rules of scaling discovered by Max Kleiber. Nature 403, 597.

Steenson, LV., Turnock, SR., Phillips, AB., Harris, C., Furlong, ME., Rogers, E., Wang, L., Bodles, K., Evans, D.W., 2014. Model predictive control of a hybrid autonomous underwater vehicle with experimental verification. In: Proceedings of the Institution of Mechanical Engineers. Part M: Journal of Engineering for the Maritime Environment 228 (2), 166–179, 10.1177/1475090213506185.

Steinhausen, M.F., Steffensen, J.F., Andersen, N.G., 2005. Tail beat frequency as a predictor of swimming speed and oxygen consumption of saithe (Pollachius virens) and whiting (Merlangius merlangus) during forced swimming. Mar. Biol. 148, 197–204.

Tanaka, H., Takagi, Y., Naito, Y., 2001. Swimming speeds and buoyancy compensation of migrating adult chum salmon Oncorhynchus keta revealed by speed/depth/acceleration data logger. J. Exp. Biol. 204, 3895–3904.

Telepraph, 2014. GhostSwimmer: US Navy trials underwater shark robot.

Townsend, C.R., Winfield, I.J., 1985. The application of optimal foraging theory to feeding behaviour in fish. In: Tyler, P., Calow, P. (Eds.), Fish Energetics: New Perspectives. Johns Hopkins University Press, Baltimore, Maryland, pp. 67–98.

Tucker, V.A., 1970. Energetic cost of locomotion in animals. Comp. Biochem. Physiol. 34 (4), 841–846.

Tudorache, C., O'Keefe, R.A., Benfey, T.J., 2011. Optimal swimming speeds reflect preferred swimming speeds of brook charr (Salvelinus fontinalis Mitchill, 1874). Fish. Physiol. Biochem. 37, 307–315.

Unmanned, 2012. University Engineers Developing Mantabot Ray AUV.

Videler, J.J., 1993. Fish Swimming. Springer, New York.

Videler, J.J., Nolet, B.A., 1990. Costs of swimming measured at optimum speed: Scale effects, differences between swimming styles, taxonomic groups and submerged and surface swimming. Comp. Biochem. Physiol. Part A: Physiol. 97 (2), 91–99.

Watanabe, Y.Y., Sato, K., Watanuki, Y., Takahashi, A., Mitani, Y., Amano, M., Aoki, K., Narazaki, T., Iwata, T., Minamikawa, S., Miyazaki, N., 2010. Scaling of swim speed in breath-hold divers. J. Anim. Ecol. 80 (1), 57–68.

Webb, P.W., 1975. Hydrodynamics and energetics of fish propulsion. Bull. Fish. Res. Board Can. 190, 1–158.

Weihs, D., 1973. Optimal fish cruising speed. Nature 245, 48–50.

White, C.R., Seymore, R.S., 2003. Mammalian basal metabolic rate is proportional to body mass2/3. Proc. Natl. Acad. Sci. USA 100 (7), 4046–4049.

Williams, C.D., 2010. A hydrodynamic basis for estimating the endurance of autonomous vehicles for mission planning. J. Ocean. Technol. 5 (3), 70–94.

Williams, R., Noren, D.P., 2009. Swimming speed, respiration rate, and estimated cost of transport in adult killer whales. Mar. Mammal. Sci. 25 (2), 327–350.

Williams, T.M., 1999. The evolution of cost efficient swimming in marine mammals: limits to energetic optimization. Philos. Trans. R. Soc. B: Biol. Sci. 354 (1380), 193–201.